Liquid Crystals
Publication details, including instructions for authors and subscription information:
http://www.informaworld.com/smpp/title~content=t713926090

Structure peculiarities and optical properties of nanocomposite: 5CB liquid crystal-CTAB-modified montmorillonite clay

T. Bezrodna[a]; I. Chashechnikova[a]; V. Nesprava[a]; G. Puchkovska[a]; Ye. Shaydyuk[a]; Yu. Boyko[b]; J. Baran[c]; M. Drozd[c]
[a] Institute of Physics of NAS Ukraine, Kyiv, Ukraine [b] Institute of Biocolloidal Chemistry of NAS Ukraine, Kyiv, Ukraine [c] Institute of Low Temperature and Structure Research, PAS, Wroclaw, Poland

Online publication date: 04 March 2010

To cite this Article Bezrodna, T. , Chashechnikova, I. , Nesprava, V. , Puchkovska, G. , Shaydyuk, Ye. , Boyko, Yu. , Baran, J. and Drozd, M.(2010) 'Structure peculiarities and optical properties of nanocomposite: 5CB liquid crystal-CTAB-modified montmorillonite clay', Liquid Crystals, 37: 3, 263 — 270
To link to this Article: DOI: 10.1080/02678290903511677
URL: http://dx.doi.org/10.1080/02678290903511677

Liquid Crystals,
Vol. 37, No. 3, March 2010, 263–270

Taylor & Francis
Taylor & Francis Group

Structure peculiarities and optical properties of nanocomposite: 5CB liquid crystal–CTAB-modified montmorillonite clay

T. Bezrodna[a], I. Chashechnikova[a], V. Nesprava[a], G. Puchkovska[a]*, Ye. Shaydyuk[a], Yu. Boyko[b], J. Baran[c] and M. Drozd[c]

[a]*Institute of Physics of NAS Ukraine, Kyiv, Ukraine;* [b]*Institute of Biocolloidal Chemistry of NAS Ukraine, Kyiv, Ukraine;* [c]*Institute of Low Temperature and Structure Research, PAS, Wroclaw, Poland*

(Received 19 June 2009; final version received 25 November 2009)

The effects of the modification of natural layered montmorillonite (MMT) clay by cetyltrimethylammonium bromide (CTAB) cations on the structure and optical properties of the composite material based on this mineral (4.5%mass) and a nematic liquid crystal (LC), 4-pentyl-4'-cyanobiphenyl (5CB), have been investigated. As shown by small-angle X-ray diffraction and infrared (IR) spectroscopy experiments, this modification results in a significant expansion of the interplane spaces in the MMT nanoparticles and a considerable growth of their surface affinity to the 5CB molecules, which allows the LC molecules to penetrate into the MMT galleries and additionally expand these galleries. According to IR studies, this heterosystem possesses van der Waals interactions between its components on the phase separation boundary and, as a result, orientation alignment of the molecules in the near-surface layers occurs. These interactions specify the electro-optical properties of the composite. When an electric field is applied to a system, the light transmittance of the material increases due to the induced orientation of the LC dimers. This LC ordering remains even after the voltage is shut off, i.e. the system shows an electro-optical memory effect.

Keywords: LC-clay nanocomposites; CTAB; montmorillonite; 5CB

1. Introduction

The investigation of the optical properties of heterogeneous systems based on liquid crystals (LCs) filled with nanoparticles of different natures and shapes is one of the important fields in modern physics. In these composites, under the influence of inorganic particles, LCs change considerably their physical characteristics, such as their optical, electro-optical (EO) and dielectric features, and their structure formation, molecule mobility etc. The materials mentioned can be used in the development of optoelectronic devices, scattering displays, information recording and storage equipment. The shape of the inorganic nanoparticles is a crucial factor that affects the physical properties of the nanocomposites. Compared to spherical nanoparticles (for example, aerosils), anisometric nanoparticles of the natural aluminosilicate montmorillonite (MMT) clay minerals (CM) have the advantage of larger contact surface area with an organic medium (in particular, with LCs), which intensifies their aligning effect on the adjacent organic layers. In order to make the Na-form CM particle surface organophilic, the CM particles are subjected to modification by polyatomic cations of organic surface-active substances (SAS) with different chemical content (see, for example, [1–5]). The nanocomposites based on the organo-modified CM nanoparticles and LCs show pronounced EO characteristics [6–8]. The EO properties of the composites containing 5CB LC and organophilic MMT nanoparticles, modified with octadecylbenzyldimethylammonium chloride (OBDM), sample B2, and dioctadecyldimethylammonium chloride (DODM), sample B3, were studied in [7,8]. The EO parameters of these materials were shown to be strongly dependent on the chemical nature of the modifier, which determined the degrees of the chemical and adsorption affinities between the inorganic surface and 5CB and influenced the structure formation processes in these composites, and, as a result, specified their EO behaviour.

In recent years, cetyltrimethylammonium bromide, CTAB, has attracted the attention of researchers as it is an efficient SAS compound. Its unique features are its very high adsorption ability and different mobility of the hydrocarbon chain. Zhu *et al.* [4] demonstrated through their investigations that the CTAB alkyl chain 'tail' is flexible even under the very dense packing of the SAS molecules. The peculiarities mentioned for this surfactant can probably provide better penetration of the LC dimers into the interlayer spaces of the organomodified clay. Adsorption studies of several cationic surfactants with different hydrocarbon chain lengths on the MMT surface revealed that the CTAB possesses the largest adsorption ability, exceeding the mineral cation-exchange capacity (CEC) by a factor of 2.5; this results from the strong hydrophobic interactions in MMT bilayers and the changes in the surface charge

*Corresponding author. Email: puchkov@iop.kiev.ua

ISSN 0267-8292 print/ISSN 1366-5855 online

DOI: 10.1080/02678290903511677
http://www.informaworld.com

[9]. The MMT modification by CTAB causes an increase in the interplane distances in CM, the values of which depend on the CTAB concentration [9–12]. Investigations of the benzene vapour adsorption on the MMT, modified by organic cations with different $(CH_2)_n$ lengths, have shown that the highest adsorption occurs at $n = 16$. In this case, the organoclay specific active surface grew five times compared to the initial MMT. Such an increase in the benzene adsorption occurs due to an expansion of the MMT galleries and a participation of the mineral inner surface in the adsorption process [13]. Zhu and Su [14] also observed a considerably larger benzene vapour sorption capacity for the CTAB-modified bentonite, compared to the unmodified CM.

Due to their high adsorption ability, CTAB-modified MMT particles can find practical applications in industry, for example, for the water purification from hazard organic wastes. In particular, the CTAB-MMT sample showed the highest adsorption activity in the adsorption investigations of Congo Red from aqueous solutions among the MMT clays, modified by alkyltrimethylammonium bromides with alkyl chains of 8, 12 and 16 carbon atoms [15].

Taking into account the unique adsorption properties of the CTAB-modified MMT clay, one can expect quite strong interphase interactions in the composite based on this mineral and 5CB LC, in their turn, affecting the EO properties of such a heterosystem. To test this suggestion, we prepared a 5CB LC–CTAB-MMT nanocomposite and investigated the organoclay structure in the initial powder and in the composite by means of a small-angle X-ray scattering (SAXS) method and the nature of the interactions on the interphase surface by infrared (IR) spectroscopy. We also investigated the EO properties of the composite obtained and carried out a comparison of the 5CB LC–CTAB-MMT properties with composites based on MMT with other surfactants.

2. Materials and methods

The nematic LC 4-pentyl-4'-cyanobiphenyl, 5CB, with a nematic–isotropic phase transition temperature of 35.7 °C was used as an organic filler for the composite. The inorganic component of the nanocomposite was a natural layered aluminosilicate CM of 2:1 structure type, MMT from the Askan deposit (Georgia). The procedures for preparation of this MMT in a Na-form (sample B1) and its modification by cationic SAS were described in [7]. The CEC value for the B1 material was equal to 97.1 meq/100 g of clay, and its specific surface was 580 $m^2\ g^{-1}$.

CTAB (Acros, 99.0%) was used as a modifier, in order to make the B1 organophobic surface organophilic. The length of a CTAB molecule equals 2.33 nm, the diameter of its 'head' is 0.48 nm and the diameter of its alkyl chain (or 'tail') is 0.39 nm. The modification by CTAB was carried out by ion substitution for Na cations by organic cations in the CTAB aqueous solution which had a concentration slightly higher than a CEC value. This condition provides 100% cation exchange and a full covering of the MMT surface by organic cations. The sample obtained as described was denoted as B4.

The 5CB + B4 (4.5%mass) nanocomposite was prepared in the presence of acetone (1%mass) for the better swelling of B4 particles and for increased compatibility with 5CB. The mixing of the sample was carried out by a UZDM-2T ultrasound dispergator [7]. When the production of the sample was complete, acetone was evaporated in air. Its absence in the final composite was controlled by IR spectroscopy.

The X-ray diffraction studies, SAXS, for the B4 sample and the composite were carried out on an AMUR small-angle diffractometer, Cu Kα radiation, in a 2θ angle range from 0.1 to 8° with a step of 0.02°. More details about the experimental conditions can be found in [16].

The IR spectra were recorded on a Bruker IFS-88 Fourier transform infrared spectrometer in a 390–4000 cm^{-1} spectral region at room temperature. The spectral resolution was 1 cm^{-1} and the number of scans taken was 64. The accuracy of the wavenumber determination was 0.02 cm^{-1} with the spectral data being treated with the use of PEAKFIT software. The B4 and CTAB powders were measured as KBr tablets and a composite sample was placed in a cell between KBr plates, with the sample layer thickness being 10 μm.

For the electro-optical measurements, a carefully mixed sample of the composite was placed between two glass plates, whose inner surfaces were covered with a thin electroconductive film of indium tin oxide. The thickness of the sample layer was determined by the diameter of spacers located between the plates ($d = 20$ μm). The ends of the cell were sealed by epoxide. A semiconductor laser (APAV, $\lambda = 0.63$ μm) was used in these experiments; the voltage range was 0–80 V and the current frequency was $f = 2$ kHz. The dependence of the light transmittance on the applied voltage was studied after the preliminary exposure of samples to an alternating electrical field, which led to good reproducibility of the obtained results.

3. Results and discussions

According to the SAXS results for the B4 powder in comparison with the B1 powder, the significant changes in the MMT structure occur under the ion-exchange substitution for Na cations by CTAB. In particular, the SAXS pattern of the B1 sample

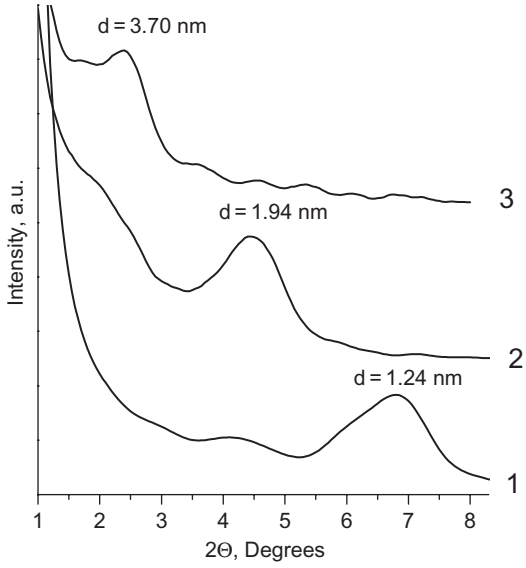

Figure 1. SAXS curves: 1 – Na-MMT (B1); 2 – CTAB-MMT (B4); 3 – 5CB+B4 composite.

contains a clear reflex, corresponding to the interplane distance $d = 1.24$ nm (Figure 1, curve 1). This value is equal to the sum of the MMT aluminosilicate packet thickness, 0.98 nm, and the diameter of the Na cation, 0.26 nm. This peak is more or less absent in the case of the B4 sample (Figure 1, curve 2), which is evidence for the total substitution of the Na ions by the organic cations. Instead of this peak, there is a pronounced reflex at $d = 1.94$ nm. This data is in a good agreement with the results of [9,10], where the X-ray diffraction experiments have been carried out for CTA^+-MMT samples with different modifier concentrations. The value obtained here for the interplane gallery gap equals 0.96 nm (i.e. 1.94–0.98 nm) and this result can correspond to a horizontal double-layer alignment of the CTA cations, for which the 'head' cross section is 0.48 nm, under the condition of an all-*trans* conformation of the C_{16} alkyl chain [10].

In contrast to the B4 sample, each SAXS graph, which we obtained earlier for the B2 and B3 powders, contains two peaks, corresponding to $d_2 = 1.8$–1.9 nm and $d_1 = 3.6$–3.9 nm. These distances give evidence for the presence of two periodic systems, due to the different alignment types of the modifier organic cations [16,17].

When the B4 nanoparticles are inserted into the 5CB LC, the SAXS pattern changes. The peak at $d = 1.94$ nm practically disappears and a new reflex of $d = 3.7$ nm arises. In other words, an abrupt expansion of the MMT galleries occurs (Figure 1, curve 3). This is certainly connected with the high adsorption ability of the CTA cations, as mentioned above, and results in the possibility of a large quantity of the 5CB dimers (2.3 nm in length, 0.5 nm in diameter) penetrating the MMT interplane spaces, significantly broadening them. This data is in agreement with the results in [2], where SAXS investigations of the suspension based on the dimethyldioctadecylammonium bromide treated Laponite particles (of 1% concentration) in 5CB are presented.

The fact that in the cases of the nanocomposites with B2 and B3 particles of 3–8%mass organoclay concentrations the expansion is observed only for the large galleries proves our conclusion that we should treat the $d_1 = 3.6$–3.9 nm peak as a separate reflex and not as a second harmonic for the $d_2 = 1.8$–1.9 nm peak [16,17]. The structure difference observed for the B4 organoclay in comparison with the B2 and B3 samples in powders and composites with 5CB can be caused by the higher adsorption ability of CTAB than those of OBDM and DODM, and, consequently, by stronger interphase interactions in the 5CB + B4 composite. This suggestion is confirmed by IR spectroscopic measurements.

The effects of the CM surface on the alignment degree of the CTAB molecules deposited on the MMT nanoparticles, and of these SAS molecules on the CM lamellae structure, have been investigated by IR spectroscopy. The character and strength of the interphase interactions between the 5CB + B4 nanocomposite components have also been determined by this method. Figure 2 presents IR spectral regions where the bands of the CTAB alkyl chain CH_2-group rocking (a) and wagging (b) vibrations are located. The CTAB is in the form of a polycrystalline powder on the MMT surface. In the case of this powder, Davydov splittings are seen for the spectral bands at 720 and 730 cm^{-1} (Figure 2(a)), and also for those at 1462 and 1473 cm^{-1} (Figure 2(b)) at room temperature. The appearance of these spectral components is connected with the peculiarities of the dense crystal packing formed by long-chain aliphatic molecules, in our case by the CTAB ones in a totally elongated conformation (*trans*-isomers), and characterised by an orthorhombic sub-cell [18,19].

The heating to $T = 90°C$ changes thermal motion of the CTAB molecules, and the alkyl chains start hindered rotations along their long axes. A transition occurs into a so-called rotator-crystalline state, which has been described in detail for another class of long-chain aliphatic compounds, normal paraffins, in [20]. Such thermal motion of the molecules leads to a distortion in the structure orientation order and a 'collapse' of the Davydov splitting components (Figure 2(a)), similar to the formation of the hexagonal structure in normal paraffins. A further temperature increase up to 120°C results in an abrupt fall of the absorption intensity in the 720–730 cm^{-1} region, where only one broad IR band is seen (Figure 2(a)). Conformation

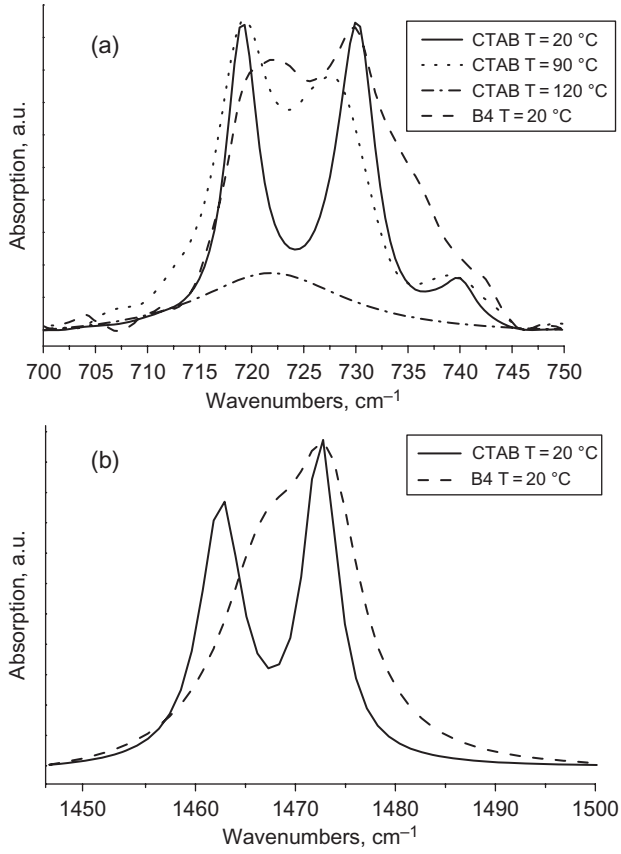

Figure 2. The IR absorption spectral regions of the alkyl CH_2-group rocking (a) and wagging (b) vibrations for the CTAB powder and the CTAB on the MMT surface.

disordering of the alkyl chains occurs at this temperature, and some of the chains transfer into a gosh-form. The so-called 'melting' of the alkyl chains occurs.

When the MMT mineral is modified, i.e. the CTAB molecules are located on the MMT surface, Davydov splitting partially collapses even at room temperature, and the whole spectral contour broadens considerably in the 720–730 and 1450–1500 cm^{-1} spectral regions (Figures 2(a) and (b)). The significant distortion of the Davydov splitting spectral components was also observed in [4] in the CTAB-MMT organoclay with a surfactant concentration corresponding to 1–1.2 CEC, where the alignment of the CTAB molecules on the MMT surface was studied as a dependence on their concentration. Such changes give evidence for the alignment distortion of the CTAB molecules in the modified MMT and the partial transition of the CTAB into a gosh-form. However, despite the conformation disordering mentioned, a certain crystal packing remains, some CTAB molecules retain their *trans*-form and the melting of the alkyl chains does not occur. In addition, the changes in the CTAB molecule conformation under the MMT modification also appear as a significant intensity redistribution for the IR bands, corresponding to the symmetric and asymmetric stretching vibrations of the alkyl chain CH_2- and CH_3-groups in the 2800–3000 cm^{-1} spectral region. This is evidently a result of changes in the local fields around the CH_2 and CH_3-groups due to the movement of the methylene chains.

Thus this data shows that the deposition of the CTAB cations on the MMT surface leads to the same result as the heating of the CTAB powder; namely, to an increase in the alkyl chain mobility (in agreement with [4]) and to their partial conformation disordering.

Figure 3 presents IR spectral regions for the O–Si–O and O–Al–O deformation (at 465 and 528 cm^{-1} for B4, and at 465 and 520 cm^{-1} for the Na-form MMT) and for Si–O stretching (at 1040 cm^{-1} for B4, and at 1010 cm^{-1} for the Na-form MMT) vibrations [11,21,22] in the clay powders and 5CB + B4 composite. The CM modification obviously shifts the peak positions of the two bands towards the high frequencies, which gives evidence for a possible decrease in the Al-O and Si-O bond lengths on the MMT lamellae surface under the influence of the modifier. Similar results were obtained in [11], where the same organoclay was investigated. When the B4 particles are added to the LC, a considerable narrowing (on 5–7 cm^{-1} of the half-width) of the 465 and 1040 cm^{-1} bands occurs, due to the aligning influence of the 5CB molecules on the organoclay lamellar structure on the phase boundary.

The IR bands of the LC molecule bond stretching and deformation vibrations change also under the influence of the B4 nanoparticles. A complex spectral band having its peaks at 813, 830, 840 and 856 cm^{-1} and corresponding to the CCH deformation vibrations of the 5CB molecules is presented in Figure 4(a).

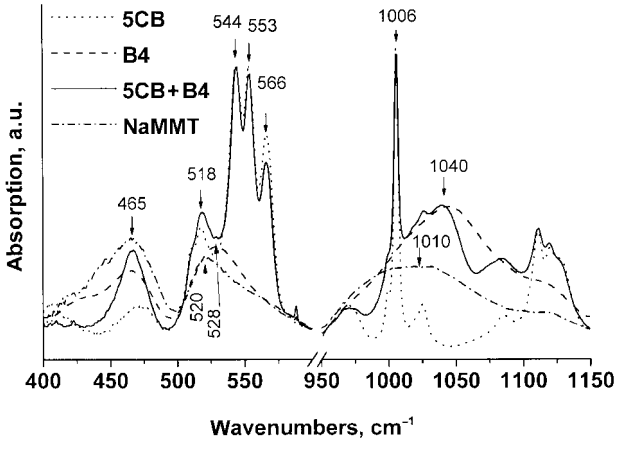

Figure 3. The IR absorption spectral regions of the O–Si–O and O–Al–O deformation (400–600 cm^{-1}) and Si–O stretching (950–1150 cm^{-1}) vibrations for the B1 and B4 powders and the 5CB+B4 composite.

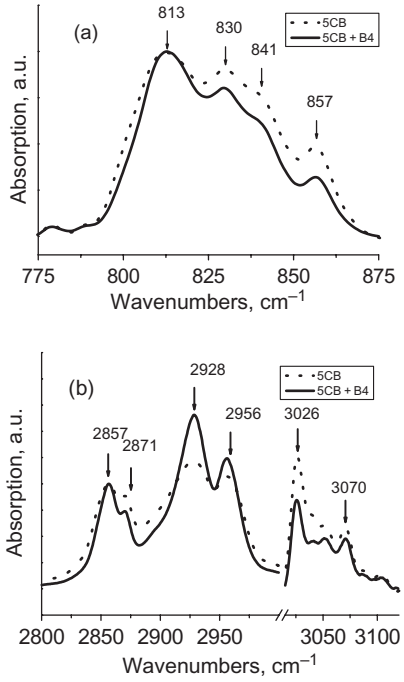

Figure 4. The IR absorption spectra of the bulk 5CB and 5CB+B4 composite: (a) a region of CCH deformation vibrations; (b) a region of CH symmetric and asymmetric stretching vibrations in the CH_2 and CH_3-groups (2800–2950 cm^{-1}) and aromatic rings (3000–3100 cm^{-1}).

Assignments of the spectral bands are made according to [4,23]. As seen from the figures, the peak positions of all of the spectral bands remain the same as for the B4 particles, but a complex band in the 775–875 cm^{-1} spectral region narrows significantly, by 7 cm^{-1} of the half-width, which is 14% (Figure 4(a)). According to the theoretical calculations [23,24], the LC 5CB compound is a mix of different conformers, appearing in the IR spectra as a set of bands in the 780–840 cm^{-1} region. The changes in the absorption intensity for this spectral region are caused by redistribution in the amounts of different 5CB molecule configurations under the influence of the B4 organoclay.

The 5CB and CTA^+ bands of the CH symmetric and asymmetric stretching vibrations in the CH_2- (2857 and 2929 cm^{-1}) and CH_3-groups (2870 and 2956 cm^{-1}) are shown in Figure 4(b). The intensity redistribution for the spectral bands at 2857, 2871, 2928 and 2956 cm^{-1} in the composites, compared to the bulk 5CB, can be the result of the changes in the dynamics of the CH_3- and CH_2-groups in the 5CB molecules, contacting with the B4 particles. At the same time, the presence of the B4 decreases the intensities of the 3026 and 3070 cm^{-1} bands, ascribed to the CH stretching vibrations of the LC benzene ring (Figure 4(b)). The mentioned intensity redistributions for the 5CB bands of the alkyl chain CH_3- and CH_2-groups and the benzene CH vibrations

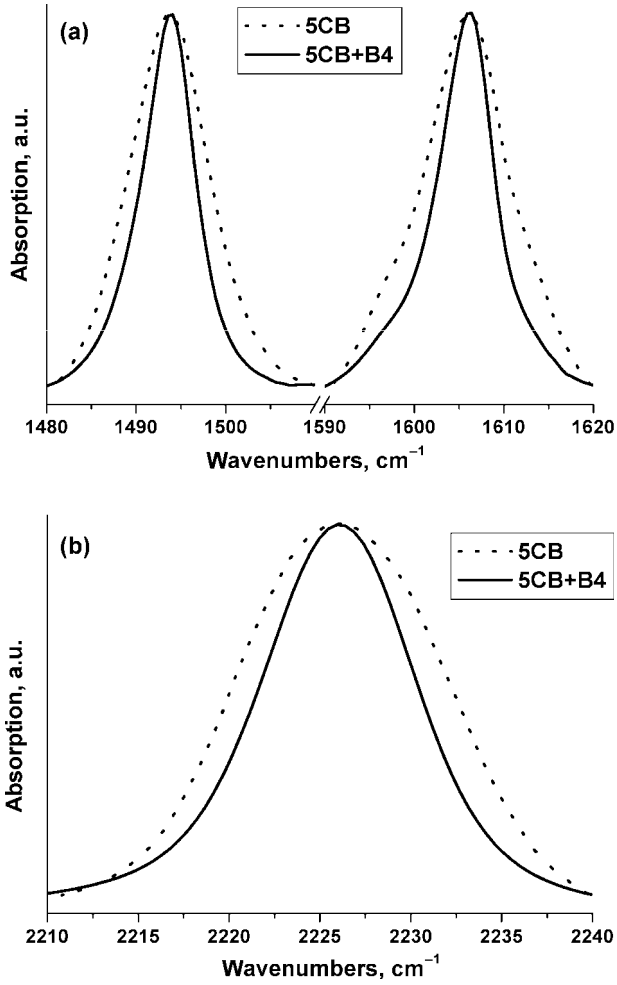

Figure 5. The IR absorption spectra of the bulk 5CB and 5CB+B4 composite: (a) regions of CCH (1480–1550 cm^{-1}) and CC (1590–1620 cm^{-1}) vibrations of the aromatic rings; (b) a region of CN-group stretching vibrations.

are probably connected with the changes in the 5CB packing on the B4 nanoparticle surface.

Figures 5(a) and (b) show the IR bands corresponding to the CCH (at 1494 cm^{-1}) and CC (at 1606 cm^{-1}) vibrations of the benzene rings, and the CN vibrations (at 2226 cm^{-1}) for the bulk 5CB and the 5CB in the composite. Retaining their spectral peak positions, the IR bands narrow significantly (by 3–4 cm^{-1} of the half-width, which is 26–36%) due to the hindrance of the 5CB molecule motions along the *x*- and *y*-axes (perpendicular to the molecule long axis) under the influence of the CM particles. The peak position of the CN band at 2226 cm^{-1} leads to the conclusion that in the composite the 5CB molecules are in a form of dipole–dipole connected dimers, as in the cases of the 5CB nematic LC phase and isotropic liquid [25].

The following fact is noticeable: the narrowing of the spectral bands in the composite with B4 nanoparticles is larger than those values with B2 [7] and B3 [8].

Table 1. The half-width narrowing of the 5CB IR bands in the 5CB + B2, B3 and B4 (4.5%mass) nanocomposites.

	5CB+B4		5CB+B2 [7]		5CB+B3 [8]	
IR band position, cm^{-1}	$\Delta\delta$*, cm^{-1}	$\Delta\delta_{rel}$**, %	$\Delta\delta$, cm^{-1}	$\Delta\delta_{rel}$, %	$\Delta\delta$, cm^{-1}	$\Delta\delta_{rel}$, %
775–875	7	14	3.7	9	1.5	3.5
1494	3.5	33	1.5	~15	1.0	12
1606	4.0	36	1.5	~15	1.0	12
2226	3.5	26	~2.0	16	1.0	6

Notes: *) $\Delta\delta = \delta_{5CB} - \delta_{(5CB+B2,\ B3\ or\ B4)}$.
**) $\Delta\delta_{rel} = \Delta\delta/\Delta\delta_{(5CB+B2,\ B3\ or\ B4)}$.

As an example, Table 1 contains the absolute ($\Delta\delta$, cm^{-1}) and relative ($\Delta\delta_{rel}$, %) values for the half-width narrowing of the IR bands in the composites with 4.5% mass of B2, B3 and B4 particles. According to this data, the 5CB + B4 composite is characterised by stronger interphase interactions and denser packing, even compared to the 5CB + B2 sample, where the π–π interactions between the benzene rings of the surfactant and liquid crystal molecules occur [17]. The results of the IR studies correlate with the X-ray experiments, showing that the loading of the B4 into 5CB leads to a more significant broadening of these organoclay interplane distances than in the cases of B2 and B3, because of the larger number of 5CB dimers incorporated.

The doublet band with spectral components at 1180 and 1186 cm^{-1} (Figure 6) corresponds to the deformation vibrations of the 5CB benzene ring CCH-groups. According to [23], a peak at 1180 cm^{-1} corresponds to the vibrations of the benzene ring, connected to an alkyl fragment of the 5CB molecule, and one at 1186 cm^{-1} is assigned to a ring close to the CN-group. The intensity values of these spectral components are more or less equal in the bulk 5CB. The intensity growth of the 1186 cm^{-1} band in the composite in comparison with the bulk 5CB can be caused by stronger interactions of this molecule fragment with the CM surface CTA cations, i.e. the 5CB molecules approach the organoclay surface exactly by the molecule fragment with CN-group. The intensity increase of this band is also observed for the 5CB+B2 composite [17], which is explained by the π–π interactions of the OBDM and 5CB benzene rings. In contrast, a relative growth of the 1180 cm^{-1} band intensity is seen in the 5CB+B3 composite [16], i.e. stronger interactions with the alkyl fragment occur; see Figure 6.

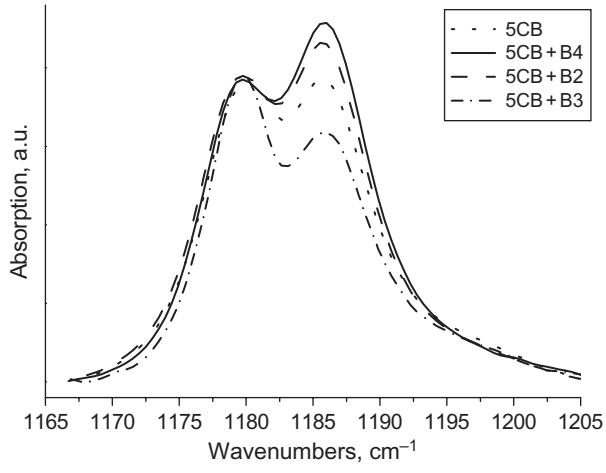

Figure 6. The IR absorption spectra in a region of CCH deformation vibrations of the 5CB aromatic rings.

To conclude, the spectral peak positions of the IR bands corresponding to the vibrations of 5CB molecules do not change, giving evidence for the absence of new chemical, hydrogen or coordination bonds in the composite. However, the considerable narrowing of the IR bands assigned to the Si–O, Al–O, CCH, C–C and CN bond vibrations results from the mutual influence (van der Waals interactions) of the 5CB + B4 composite components on the interphase boundary, appearing in the alignment of the LC and CM near-surface layers. These effects are much stronger in the heterosystem with the B4 nanoparticles than in the heterosystems with B2 and B3 (Table 1).

Based on the data obtained by IR spectroscopy and SAXS methods, one can suggest reasons for the higher adsorption ability (in particular, to 5CB) of the MMT modified by CTAB in comparison with other SAS (for example, OBDM and DODM). A steric factor can play a significant role in the sample with CTAB. According to the IR spectroscopic investigations, the 5CB molecules approach the B4 surface by a fragment containing a nucleophilic CN-group. Due to the electrostatic interactions, it attracts the N^+-ion of the modifier molecule. In contrast to the complex OBDM and DODM molecules, in the CTAB this cation is connected only with one quite movable hydrocarbon chain, C_{16}. Consequently, a larger number of the 5CB molecules can approach the B4 surface, resulting in a more considerable expansion of the organoclay galleries in 5CB ($d_{B4} = 1.94$ nm, $d_{5CB+B4} = 3.7$ nm) when

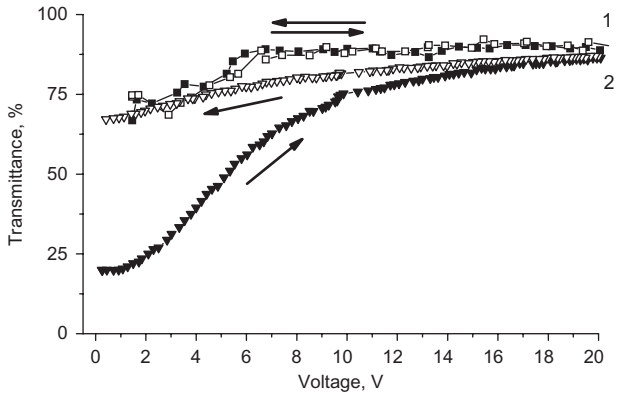

Figure 7. The transmittance dependence on the voltage: 1 – the bulk 5CB; 2 – the 5CB+B4 composite. The voltage growth is marked with dark symbols; the light symbols represent the regime of voltage decrease.

compared with the B2 and B3 particles and, correspondingly, in the stronger interphase interactions and narrower IR bands.

The quite strong interphase interactions in the 5CB + B4 composite should be reflected in its EO properties. We studied the dependencies of the light transmittance on the voltage applied and compared the result with those for the bulk 5CB (Figure 7). The memory effect, M, and contrast, K, were calculated using the following equations:

$$M = \frac{T_m - T_o}{T_{sat} - T_o} \times 100\%, \quad (1)$$

$$K = \frac{T_{sat}}{T_o}, \quad (2)$$

where T_o is the initial light transmittance, T_m is the residual light transmittance and T_{sat} is the maximum light transmittance at the saturation voltage, U_{sat}. It should be noted that information display devices need quite a large value of K and a large memory effect is necessary for information recording and storage equipment.

As seen from Figure 7, the transmittance of the bulk 5CB does not depend on the voltage value above 5 V, and the system is reversible ($M = 0$, $K = 1$). In the case of the 5CB + B4 composite, transmittance saturation is achieved even at 17 V and the memory effect equals 69%.

Table 2 lists the results of the EO investigations for different composites with the organoclay nanoparticles, B4, B2 [7] and B3 [8], produced by the same procedure (with acetone addition) at the CM concentration of 4.5%mass. According to this data, T_o has its maximum value in the 5CB + B4 composite and here T_{sat} is achieved at the smallest voltage compared to the other CMs. This last fact can be explained by the larger number of 5CB dimers, contacting the B4 nanoparticles, as seen from the IR spectroscopy and X-ray experiments. Therefore, the composite components are more easily re-orientated along the electric field and the material reaches its most transparent state at a lower U_{sat}. Moreover, this material is characterised by a quite high residual light transmittance, T_m, and high memory. According to [26], the affinity level of the organoclay surface to LC molecules is proportional to T_m. This value is largest for the 5CB + B4 composite, i.e. the strongest interphase interactions occur in this heterosystem compared to the composites with B2 and B3 particles. The data mentioned is in a good agreement with our IR spectroscopic results, where the largest narrowing of the spectral bands of both the B4 organoclay and 5CB dimers is observed in the case of the 5CB + B4 composite.

Table 2. EO properties of the composites based on the 5CB and organoclays (4.5%mass).

Composite	T_o, %	T_{sat}, %	T_m, %	U_{sat}, V	M, %	K
5CB + B4	20	88	67	17	69	~ 5
5CB + B2 [7]	4	75	58	55	76	18
5CB + B3 [8]	~ 0.2	55	4	38	7	~ 300

4. Conclusions

This investigation has shown that the MMT modification by the CTAB surfactant results in an abrupt increase of the adsorption affinity level of the CM surface to the 5CB molecules. The loading of the B4 particles with LC leads to a significant expansion of the aluminosilicate interpacket space due to the penetration of a large quantity of 5CB dimers. The contact area between the LC medium and CM nanoparticles grows, and the dispersion of these particles in the composite becomes better. According to the analysis of the IR spectroscopic data, van der Waals interactions occur between the components of such a heterosystem on the interphase boundary; they result in the alignments of the molecules in the near-surface layers. When a voltage is applied to this material, due to the quite strong interphase interactions, the LC domains and CM nanoparticles orientate along the electric field and the composite light transmittance increases. Removal of the voltage does not disorder the aligned state of the system and a memory effect is observed.

The EO investigations of the 5CB + B4 composite together with the data from [7,8], where the MMT surfactants are OBDM and DODM, confirm the conclusion that the variation of the organoclay surface

chemical content allows control of the affinity level between the LC and CM, and, consequently, composites with 5CB with a wide range of EO properties can be obtained.

Acknowledgements

This work was partially funded by the NAS of Ukraine under the Program 'Nanophysics and Nanoelectronics', project VC-138. The authors would like to thank Dr N. Lebovka and A. Tolochko for their help in these investigations.

References

[1] Hackman, I.; Hollaway, L. *Composites: Part A* **2006**, *37*, 1161–1170.
[2] Pizzey, C.; Klein, S.; Leach, E.; van Duijneveldt, J.S.; Richardson, R.M. *J. Phys.: Condens. Matter* **2004**, *16*, 2479–2495.
[3] van Duijneveldt, J.S.; Klein, S.; Leach, E.; Pizzey, C.; Richardson, R.M. *J. Phys.: Condens. Matter* **2005**, *17*, 2255–2267.
[4] Zhu, J.; He, H.; Zhu, L.; Wen, X.; Deng, F. *J. Colloid Interface Sci.* **2005**, *286*, 239–244.
[5] Zhang, Z.; Duijneveldt, J. *Soft Matter* **2007**, *3*, 596–604.
[6] Kawasumi, M.; Usuki, A.; Okada, A.; Kurauchi, T. *Mol. Cryst. Liq. Cryst.* **1996**, *281*, 91–103.
[7] Chashechnikova, I.; Dolgov, L.; Gavrilko, T.; Puchkovska, G.; Shaydyuk, Y.; Lebovka, N.; Moraru, V.; Baran, J.; Ratajczak, H. *J. Mol. Struct.* **2005**, *744–747*, 563–571.
[8] Bezrodna, T.; Chashechnikova, I.; Dolgov, L.; Puchkovska, G.; Shaydyuk, Y.; Lebovka, N.; Moraru, V.; Baran, J.; Ratajczak, H. *Liq. Cryst.* **2005**, *32*, 1005–1012.
[9] Shang, C.; Rice, J.; Lin, J. *Soil Sci. Soc. Am. J*. **2002**, *66*, 1225–1230.
[10] Zheng, Q.; Hu, B.; Song, Y.; Yang, H.; Pan, Y. *J. Mater. Res.* **2005**, *20*, 357–363.
[11] Praus, P.; Turicova, M.; Študentova, S.; Ritz, M. *J. Colloid Interface Sci.* **2006**, *304*, 29–36.
[12] Zhu, L.; Zhu, R.; Xu, L.; Ruan, X. *Colloids Surf., A* **2007**, *304*, 41–48.
[13] Moraru, V. Investigations of Organoclay Structure and Surface Properties. Doctorial Thesis, Institute of Colloid Chemistry, NAS of Ukraine, Kiev, 1970 (in Russian).
[14] Zhu, L.; Su, Y. *Clays Clay Miner.* **2002**, *50*, 421–427.
[15] Wang, L.; Wang, A. *J. Hazard. Mater.* **2008**, *160*, 173–180.
[16] Bezrodna, T.; Chashechnikova, I.; Puchkovska, G.; Tolochko, T.; Shaydyuk, Y.; Lebovka, N.; Baran, J.; Drozd, M.; Ratajczak, H. *Liq. Cryst.* **2006**, *33*, 1113–1119.
[17] Bezrodna, T.; Chashechnikova, I.; Gavrilko, T.; Puchkovska, G.; Shaydyuk, Y.; Tolochko, T.; Baran, J.; Drozd, M. *Liq. Cryst*. **2008**, *35*, 265–274.
[18] Babkov, L.; Puchkovska, G.; Makarenko, S; Gavrylko, T. *IR-spectroscopy of molecular crystals with hydrogen bonds*, Naukova dumka, Kiev, 1989 (in Russian).
[19] Vand, V. *Acta Crystallogr*. **1951**, *4*, 104–105.
[20] Puchkovska, G.; Danchuk, V.; Kravchuk, A.; Kukelski, J. *J. Mol. Struct*. **2004**, *704*, 119–123.
[21] Lazarev, A. *Vibrational Spectra and the Structure of Silicates*. Nauka: Leningrad, 1968 (in Russian).
[22] Tarasevich, Y.; Ovcharenko, F. *Adsorption on the Clay Compound*. Naukova dumka: Kiev, 1975 (in Russian).
[23] Babkov, L.; Gnatyuk, I.; Puchkovska, G.; Truhachev, S. *J. Strukt. Himii* **2002**, *43,* 1098–1105 (in Russian).
[24] Tanaka, S.; Kato, C.; Horie, K. *J. Mol. Struct*. **2005**, *735–736*, 27–37.
[25] Chandrasekar, S. *Liquid Crystals*. Cambridge University Press: Cambridge, 1977.
[26] Kawasumi, M.; Hasegawa, N.; Usuki, A.; Okada, A. *Mater. Sci. Eng*. **1998**, *C6*, 135–143.